Molecular mechanism underlying juvenile hormone-mediated repression of precocious larval–adult metamorphosis

Takumi Kayukawa[a,1], Akiya Jouraku[a], Yuka Ito[a], and Tetsuro Shinoda[a]

[a]Institute of Agrobiological Sciences, National Agriculture and Food Research Organization, Tsukuba 305-8634, Japan

Edited by Lynn M. Riddiford, University of Washington, Friday Harbor, WA, and approved December 16, 2016 (received for review September 16, 2016)

Juvenile hormone (JH) represses precocious metamorphosis of larval to pupal and adult transitions in holometabolous insects. The early JH-inducible gene *Krüppel homolog 1* (*Kr-h1*) plays a key role in the repression of metamorphosis as a mediator of JH action. Previous studies demonstrated that Kr-h1 inhibits precocious larval–pupal transition in immature larva via direct transcriptional repression of the pupal specifier *Broad-Complex* (*BR-C*). JH was recently reported to repress the adult specifier gene *Ecdysone-induced protein 93F* (*E93*); however, its mechanism of action remains unclear. Here, we found that JH suppressed ecdysone-inducible *E93* expression in the epidermis of the silkworm *Bombyx mori* and in a *B. mori* cell line. Reporter assays in the cell line revealed that the JH-dependent suppression was mediated by Kr-h1. Genome-wide ChIP-seq analysis identified a consensus Kr-h1 binding site (KBS, 14 bp) located in the *E93* promoter region, and EMSA confirmed that Kr-h1 directly binds to the KBS. Moreover, we identified a C-terminal conserved domain in Kr-h1 essential for the transcriptional repression of *E93*. Based on these results, we propose a mechanism in which JH-inducible Kr-h1 directly binds to the KBS site upstream of the *E93* locus to repress its transcription in a cell-autonomous manner, thereby preventing larva from bypassing the pupal stage and progressing to precocious adult development. These findings help to elucidate the molecular mechanisms regulating the metamorphic genetic network, including the functional significance of *Kr-h1*, *BR-C*, and *E93* in holometabolous insect metamorphosis.

metamorphosis | juvenile hormone | E93 | Krüppel homolog 1 | holometabolous insects

Holometabolous insects undergo a complete metamorphosis, which consists of egg, larval, pupal, and adult stages. Larval–pupal and pupal–adult metamorphoses are coordinated by the actions of ecdysteroids and juvenile hormone (JH) (1). In the presence of JH, 20-hydroxyecdysone (20E; the active metabolite of ecdysteroids) induces larval–larval molting, whereas, in the absence of JH, it induces larval–pupal and pupal–adult molts (1). Thus, the major function of JH is to prevent immature larvae from precociously transitioning to pupae and adults (1).

The molecular action of 20E in target cells during the larval–pupal transition was initially proposed in the 1970s (2), and its molecular mechanisms were well characterized by later studies. In particular, the 20E-liganded ecdysone receptor (EcR)/ultraspiracle (USP) complex directly activates the expression of a few early ecdysone-inducible transcription factors, which then regulate a large number of late ecdysone-inducible genes involved in pupal formation (3–5). The molecular mechanism of JH signaling has been clarified more recently (6–8). The JH receptor methoprene tolerant (Met) was found to bind JH (9–12) and subsequently interact with steroid receptor coactivator (SRC; also known as FISC and Taiman) (13–15). The JH/Met/SRC complex then activates *Krüppel homolog 1* (*Kr-h1*) (15, 16), which plays a key role in the repression of metamorphosis (17–20).

The transcription factor Broad-Complex (BR-C), which consists of a Bric-a-brac/Tramtrack/Broad complex and zinc finger domains, is induced by 20E and functions as a "pupal specifier" during the larval–pupal transition (21–24). An amorphic *BR-C* mutant of *Drosophila melanogaster* failed to achieve larval–pupal metamorphosis (22, 23), and overexpression of *BR-C* in penultimate-instar larvae concomitantly suppressed the expression of larval cuticle genes and activated pupal cuticle genes (24). *Kr-h1* is required for *BR-C* repression in the fat body in *D. melanogaster* (25). In Lepidoptera, JH was shown to repress 20E-dependent induction of *BR-C* in the larval epidermis (26, 27). We have found that Kr-h1 directly binds to a site within the *BR-C* promoter and represses 20E-dependent *BR-C* activation (28). Through these molecular actions, JH prevents immature larvae from undergoing precocious larval–pupal transition.

Ecdysone-induced protein 93F (*E93*; also known as *Eip93F*), originally identified as an ecdysone-induced gene from *D. melanogaster*, is a member of the helix–turn–helix transcription factor family (29). E93 regulates the expression of genes involved in programmed cell death, including apoptosis and autophagy, to facilitate the remodeling of larval to adult tissues (30–33). A recent study in the hemimetabolous German cockroach, *Blattella germanica*, identified that *E93* is an "adult specifier gene" because cockroaches treated with *E93*RNAi continuously repeated nymphal molts and finally reached the 10th instar, whereas normal cockroaches progress through only six nymphal instars before adult metamorphosis (34). Similarly, *E93*RNAi prevented the pupal–adult transition and resulted in a supernumerary pupa in

Significance

Juvenile hormone (JH) intricately controls molting and metamorphosis in holometabolous insects. *Ecdysone-induced protein 93F* (*E93*) functions as an adult specifier gene in the pupal–adult transition. JH is known to repress *E93* expression to prevent immature larvae from bypassing the pupal stage and progressing to precocious adult development; however, the molecular mechanism underlying JH-mediated *E93* repression remains unknown. Here, we demonstrated that JH-inducible Krüppel homolog 1 functions as a direct transcriptional repressor of *E93*. This study markedly advances the present understanding of the molecular basis of JH function in repressing insect metamorphosis.

Author contributions: T.K. designed research; T.K. and Y.I. performed research; T.K. and A.J. analyzed data; and T.K., A.J., and T.S. wrote the paper.

The authors declare no conflict of interest.

This article is a PNAS Direct Submission.

Freely available online through the PNAS open access option.

Data deposition: The sequences reported in this paper have been deposited in the DDBJ/EMBL/GenBank database [accession nos. LC177616 (*BmE93A*) and LC177617 (*BmE93B*)].

[1]To whom correspondence should be addressed. Email: kayu@affrc.go.jp.

This article contains supporting information online at www.pnas.org/lookup/suppl/doi:10.1073/pnas.1615423114/-/DCSupplemental.

DEVELOPMENTAL BIOLOGY

Tribolium castaneum and *D. melanogaster*, suggesting that the function of *E93* as an adult specifier gene is conserved in holometabolous insects (34).

A recent analysis demonstrated that *E93* expression is induced by 20E and repressed by JH similarly to *BR-C* (34). Moreover, it was first reported in *B. germanica* that JH-inducible Kr-h1 suppressed *E93* transcript levels (35), and this effect was also observed in *D. melanogaster* and *T. castaneum* (36); however, these findings were obtained mainly by RNAi-based genetic analyses using individual insects, and therefore the molecular mechanism underlying JH-mediated repression of *E93* in the cells remains poorly understood. In particular, it is unknown whether Kr-h1 represses *E93* transcription directly or indirectly, and how Kr-h1 represses the transcript of *E93*. Therefore, in this study, we sought to elucidate this molecular mechanism in *Bombyx mori*, and proposed that JH prevents precocious larval–adult metamorphosis via direct Kr-h1–dependent *E93* gene repression.

Results

Genomic Structure and Expression Profile of *E93* in Vivo and in a Cell Line. Two *BmE93* isoforms with different transcription start sites, *BmE93A* (LC177616) and *BmE93B* (LC177617), were identified by rapid amplification of 5′ cDNA ends (5′RACE; Fig. 1*A*). *BmE93A* and *BmE93B* had partially different 5̃′UTRs but shared a common ORF (Fig. 1*A*). Comparison of the cDNA sequences to the *B. mori* genome database (37) revealed that the transcription start site of *BmE93B* was located downstream of that of *BmE93A* (Fig. 1*A*).

Developmental changes in *BmE93A/B* expression in the epidermis of *B. mori* were determined by quantitative PCR (qPCR; Fig. 1*B*). Only trace expression of the two isoforms was detected in the fifth instar stage (Fig. 1*B*), but gradually increased toward the pupal stage (Fig. 1*B*, *Inset*). *BmE93A* transcript levels peaked at day 0 of the pupal stage and diminished thereafter, whereas the *BmE93B* transcript was expressed at low levels during the pupal stage and its levels peaked during the adult stage (Fig. 1*B*). Little difference was observed in the expression of both isoforms between females and males. Notably, the expression patterns of *BmE93A* and *BmE93B* were dominant in the pupal and adult stages, respectively. The expression pattern of *BmE93A* was highly correlated with the changes in hemolymph ecdysteroid titer (38–41) when *BmKr-h1* expression was absent (15, 42) (Fig. 1*B*), suggesting that *BmE93A* was induced by 20E and suppressed by BmKr-h1.

Following this result, we examined the effect of 20E and methoprene [a JH analog (JHA)] on the cultured epidermis of pupae at day 0. *BmE93A* expression of pupa at day 0 was induced by 20E, and JHA repressed this induction; however, these hormones had little effect on *BmE93B* transcription (Fig. 1*C*). Our previous studies showed that JHA induced *BmKr-h1* expression in the epidermis of fifth-instar larvae at day 5 and adults at day 0 (42). Consistently, JHA also induced *BmKr-h1* expression in day 0 pupae, and 20E superinduced it (Fig. 1*C*).

Next, we examined the hormonal regulation of *BmE93* transcripts in a *Bombyx* cell line (NIAS-Bm-aff3 cells) by qPCR. The *BmE93A* transcript was weakly detectable at baseline, but it was significantly up-regulated by 20E, and this effect was repressed by JHA (Fig. 1*D*). The responses to these hormones were weaker for *BmE93B* transcripts than for *BmE93A* transcripts (Fig. 1*D*).

Identification of *cis* and *trans* Elements Involved in JH-Dependent *BmE93A* Repression. A previous study demonstrated that BmKr-h1 directly binds to a Kr-h1 binding site (KBS) in the *BmBR-C* promoter and represses 20E-dependent *BmBR-C* transcription (28). Thus, we hypothesized that BmKr-h1 is also involved in the JH-mediated repression of *BmE93A*. To test this hypothesis, we searched for sequences with shared similarity to the *BmBR-C* KBS upstream of *BmE93A* (<3 kb), and found a candidate KBS (−2221 to −2208) that was highly similar to the *BmBR-C* KBS (Fig. 2*A*). Interestingly, a putative ecdysone response element (EcRE; −2179 to −2167) that was homologous to a consensus EcRE sequence (RGKTCANTGAMCY) (43) was located near

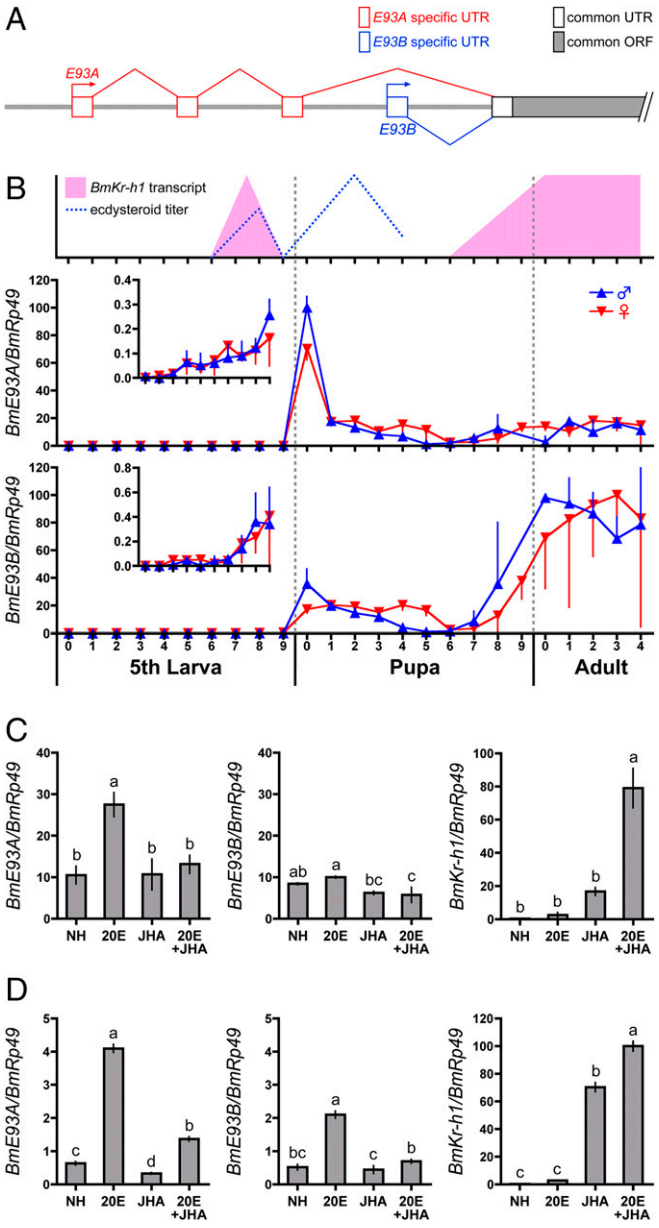

Fig. 1. Gene structure, developmental profile, and hormonal regulation of *BmE93*. (*A*) Schematic representation of the *BmE93* gene structure. Predicted exons are shown as boxes. The *BmE93* gene has two transcriptional start sites [the distal promoter (*BmE93A*, red) and the proximal promoter (*BmE93B*, blue)]. (*B*) Developmental expression profiles of *BmE93A* and *BmE93B* in the epidermis of *B. mori* as determined by qPCR. The numbers under the horizontal axis indicate the days in the respective stage. Blue and red triangles indicate males and females, respectively. (*Inset*) Vertical axes are scaled to show expression changes at low levels. The changes in the ecdysteroid titer and *BmKr-h1* transcripts are depicted based on the data from previous studies. (*C*) Integuments of day 0 pupae were cultured in the presence of 1 μM 20E and 10 μM JHA for 1 d, and expressions of *BmE93A*, *BmE93B*, and *BmKr-h1* were monitored. (*D*) *BmE93A*, *BmE93B*, and *BmKr-h1* expression were examined in NIAS-Bm-aff3 cells treated with 1 μM 20E and 10 μM JHA for 1 d. The transcript levels of *BmE93A* in male pupae at day 0, *BmE93B* in adult males at day 0, and *BmKr-h1* in NIAS-Bm-aff3 cells treated with 20E and JHA were set as 100. The data represent means ± SD (n = 3–4). Bars with the same letter (*C* and *D*) are not significantly different (Tukey–Kramer test, $\alpha = 0.05$).

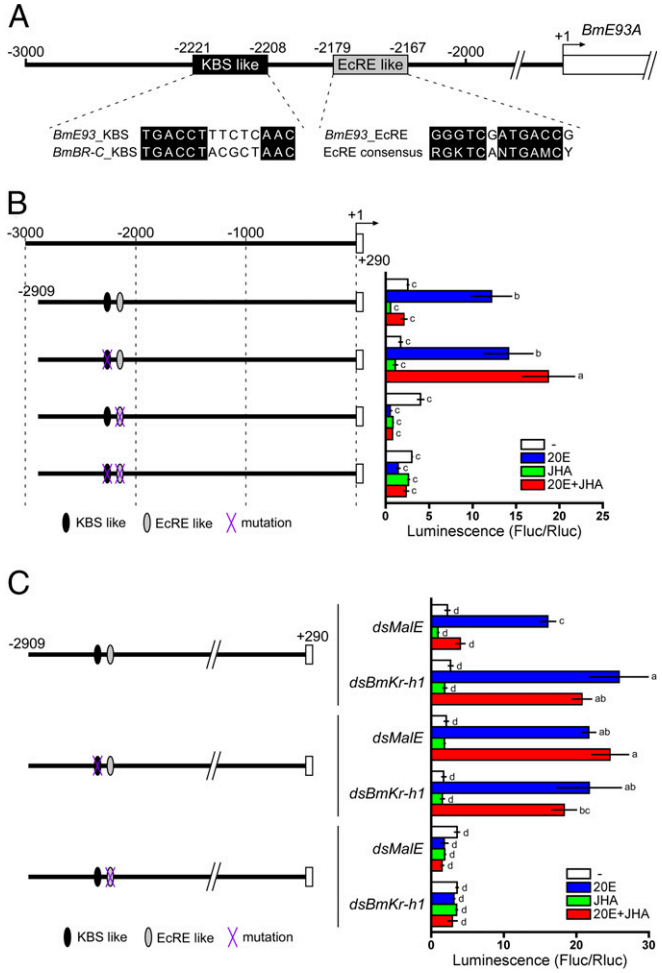

Fig. 2. Identification of the BmKBS and EcRE in the *BmE93A* promoter region. (*A*) The predicted KBS and EcRE in the *BmE93A* promoter region. The numbers indicate the distance from the *BmE93A* transcription start site. The putative KBS and EcRE are aligned with the KBS of *BmBR-C* and EcRE consensus sequences, respectively. (*B*) Functional characterization of the putative KBS and EcRE in *BmE93A*. NIAS-Bm-aff3 cells were cotransfected with reporter plasmids carrying the promoter regions indicated in the figure and a reference reporter plasmid. Cells were treated with 1 μM 20E and 10 μM JHA for 2 d, and reporter activity was measured by using a dual-luciferase reporter assay system. Data represent means ± SD (n = 3). Bars with the same letter are not significantly different (Tukey–Kramer test, $\alpha = 0.05$). Black and gray ellipses indicate the KBS sequence (−2221 to −2208) and EcRE sequence (−2179 to −2167), respectively. The purple "X" indicates a mutated sequence. (*C*) Functional interaction of KBS and BmKr-h1. NIAS-Bm-aff3 cells were cotransfected with reporter plasmids, a reference reporter plasmid, and *dsBmKr-h1* or *dsMalE* (control) and then treated with 20E or JHA. Other procedures were identical to those in *B*.

the putative KBS (Fig. 2*A*), whereas the upstream region of *BmE93B* (<3 kb) did not contain this consensus sequence. To characterize the function of the putative KBS and EcRE at the *BmE93A* locus, we performed reporter assays in NIAS-Bm-aff3 cells using constructs carrying the −2909 to +290 region of *BmE93A* with or without mutations in these sequences. The WT *BmE93A* reporter was strongly activated by 20E, and this induction was completely repressed by JHA (Fig. 2*B*). Mutation in the putative KBS region abolished this JHA-dependent repression (Fig. 2*B*). Deletion of the putative EcRE from the WT reporter abolished 20E-induced expression (Fig. 2*B*), indicating that the sequence represents an authentic EcRE. Collectively, these results revealed that the *BmE93A* transcription was activated by 20E via the EcRE, and that the 20E-induction was repressed by JHA via the putative KBS.

To examine whether BmKr-h1 interacts with the putative KBS in *BmE93A*, we performed reporter assays in combination with RNAi. *BmKr-h1*RNAi silencing abolished JHA-dependent repression of *BmE93A* in the transcript levels (Fig. S1). Notably, *BmKr-h1*RNAi alleviated the JHA-dependent reporter suppression (Fig. 2*C*), whereas treatment with *dsMalE* (RNAi control) had no effect on reporter activity (Fig. 2*C*), indicating that BmKr-h1 is involved in the repression of 20E-induced *BmE93A* transcription. Based on these results, we concluded that the KBS (−2221 to −2208; 14 bp) of *BmE93A* is indeed an authentic KBS that functionally interacts with BmKr-h1.

Conservation of the KBS. To identify the putative KBSs on a genome-wide basis, we performed ChIP-seq analysis using BmN cells overexpressing BmKr-h1 with a C-terminal HA or V5 epitope tag (BmKr-h1_HA tag and BmKr-h1_V5 tag, respectively). Focusing on the region around the *BmE93A* locus (2708–2711.5-kbp region in Bm_Scaf25), 10 peaks enriched with read sequences were observed in input samples of BmN cells overexpressing BmKr-h1_HA tag and BmKr-h1_V5 tag (Fig. 3*A*). An enriched peak between 2708.0 and 2708.5 kbp was observed in both ChIP products (Fig. 3*A*, red box), and this region contained the KBS identified in this study (Fig. 3*A*). We designed ChIP-qPCR primers to determine the quantities of enriched read sequences (Fig. 3*B*, red lines), and confirmed a significant enrichment in the region containing the KBS (Fig. 3*B*). Moreover, genome-wide motif analysis of the enriched sequences successfully identified a KBS consensus sequence (TGACCTNNNNYAAC; Fig. 3*C*). The KBSs found upstream of *BmE93A* and *BmBR-C* (28) are highly similar to the consensus KBS (Fig. 3*C*), further confirming that BmKr-h1 indeed interacts with these KBS sequences. This KBS consensus was not found in the upstream region of *BmE93B* (<3 kb).

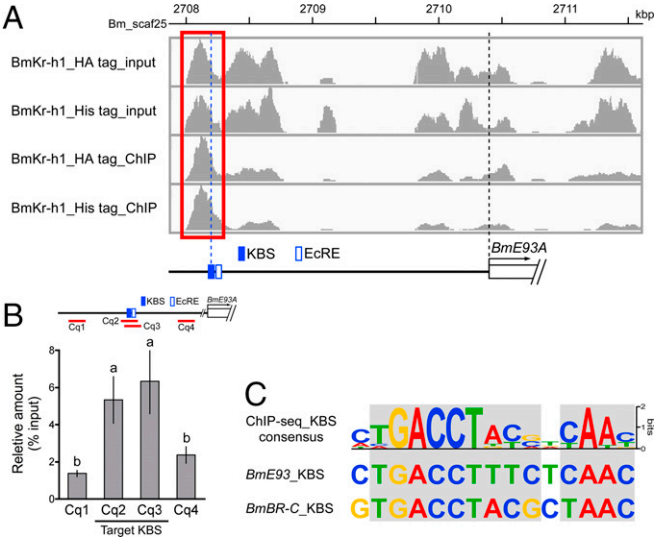

Fig. 3. KBS characterization by ChIP-seq. ChIP-seq was performed by using anti-HA and -V5 tag antibodies in BmN cells overexpressing tagged BmKr-h1. (*A*) Peak calls in the promoter region of *BmE93A* (Bm_scaf25: 2708–2711.5 kbp, chromosome 26). The red box indicates a putative ChIP-specific enriched region with the KBS and EcRE locations identified in Fig. 2 shown below. (*B*) Enrichment of the *BmE93A* KBS was quantified by ChIP-qPCR. Red lines represent the region amplified by ChIP-qPCR. The Cq2 (−2269 to −2171) and Cq3 (−2265 to −2167) regions contain the KBS, and Cq1 (−3945 to −3842) and Cq4 (−1483 to −1335) regions serve as negative controls. The data represent means ± SD (n = 4). Bars with the same letter are not significantly different (Tukey–Kramer test, $\alpha = 0.05$). (*C*) Motif analysis based on BmKr-h1 ChIP-seq. The obtained KBS consensus is aligned with that of *BmE93A* and *BmBR-C*. Light gray shading indicates highly conserved nucleotides.

DEVELOPMENTAL BIOLOGY

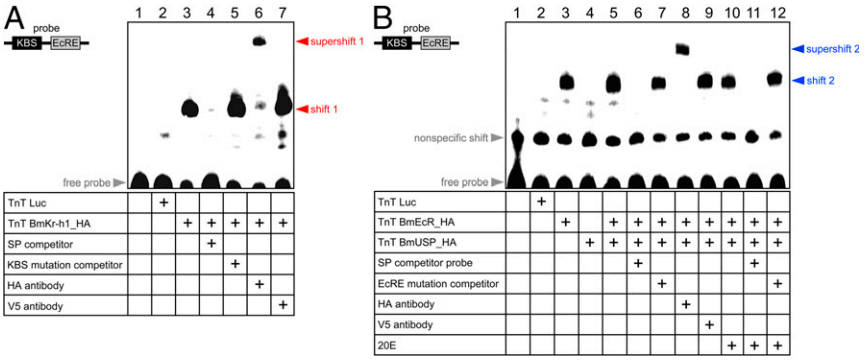

Fig. 4. BmKr-h1 directly binds to the KBS. The BmKr-h1/KBS (*A*) and BmEcR/EcRE interactions (*B*) were examined by EMSA. Luciferase (mock), BmKr-h1_HA, BmEcRE_HA, and BmUSP_HA proteins were synthesized with an in vitro transcription and translation system and incubated with biotin-tagged oligonucleotide probes (60 bp) containing the KBS and EcRE sequences. Competition assays were performed by using a 100-fold molar excess of unlabeled specific, (*A*) KBS-, or (*B*) EcRE-mutated probes. The specificity of the shifted bands was verified by using polyclonal antibodies against the HA and V5 tags (negative control).

BmKr-h1 Directly Binds to KBS. To demonstrate that BmKr-h1 directly binds to the *BmE93A* KBS, we performed EMSAs using a probe containing the KBS and EcRE sequences. As shown in Fig. 4*A*, a specific shift band appeared (shift 1) when HA-tagged BmKr-h1 (BmKr-h1_HA) was added to the probe (Fig. 4*A*, lane 3), whereas no shift band was observed when luciferase was added as a mock binding factor (negative control; Fig. 4*A*, lane 2). Competition assays showed that the specific band disappeared with the addition of a 100-fold molar excess of unlabeled probe (Fig. 4*A*, lane 4), but not KBS-mutated probe (Fig. 4*A*, lane 5, and Table S1). Moreover, the specific band supershifted in the presence of an anti-HA tag antibody (Fig. 4*A*, lane 6), but not an anti-V5 tag antibody (negative control; Fig. 4*A*, lane 7). These results clearly indicate that BmKr-h1 directly and specifically bound to the KBS sequence.

Next, we tested the interaction between BmEcR/USP and EcRE by EMSA (Fig. 4*B*). A specific shift band (shift 2) appeared when HA-tagged BmEcR (BmEcRE_HA) and BmUSP (BmUSP_HA) were added to the probe (Fig. 4*B*, lane 5), which supershifted with the addition of the anti-HA antibody (Fig. 4*B*, lane 8). This shift was not changed by the addition of 20E (Fig. 4*B*, lanes 10–12). These results reveal that BmEcR specifically binds to the *BmE93A*EcRE irrespective of the presence of 20E. Curiously, shift 2 was observed on addition of BmEcR alone (Fig. 4*B*, lane 3), implying that BmEcR alone can bind to the *BmE93A*EcRE. However, the possibility remains that a remnant USP in the cell extract of the TnT protein expression kit (derived from the *Spodoptera frugiperda* Sf21 cell line) formed a functional complex with BmEcR and bound the EcRE.

Molecular Mechanism of Transcriptional Repression by BmKr-h1. The aforementioned results facilitate us to explore the mechanism how BmKr-h1 represses the 20E-mediated *BmE93A* induction. Because the KBS and EcRE in the *E93* promoter region were separated by only 28 bp (Fig. 2*A*), we hypothesized that binding of BmKr-h1 to the KBS sterically inhibits the interaction between BmEcR and EcRE. We verified this hypothesis by using EMSA with an oligonucleotide probe that contained the KBS and EcRE sequences in *BmE93A* (Fig. 5 *A* and *B*). Specific shift bands, shift K1 and shift E1, appeared with the addition of BmKr-h1_HA (Fig. 5*A*, lane 3) and BmEcR_HA (Fig. 5*A*, lane 4), respectively. The combination of BmKr-h1_HA and BmEcR_HA resulted in a new band (shift KE1) with a lower mobility than shift K1 and E1 (Fig. 5*A*, lane 5). The shift K1 and KE1 disappeared and were supershifted by the anti-HA tag antibody (Fig. S2), suggesting that shift K1, shift KE1, supershift K1, and supershift KE1 were composed of BmKr-h1, BmKr-h1/BmEcR, BmKr-h1/antibody, and BmKr-h1/BmEcR/antibody, respectively. By using a probe lacking KBS (Fig. 5*B*), no specific shift band was observed with BmKr-h1_HA (Fig. 5*B*, lane 3),

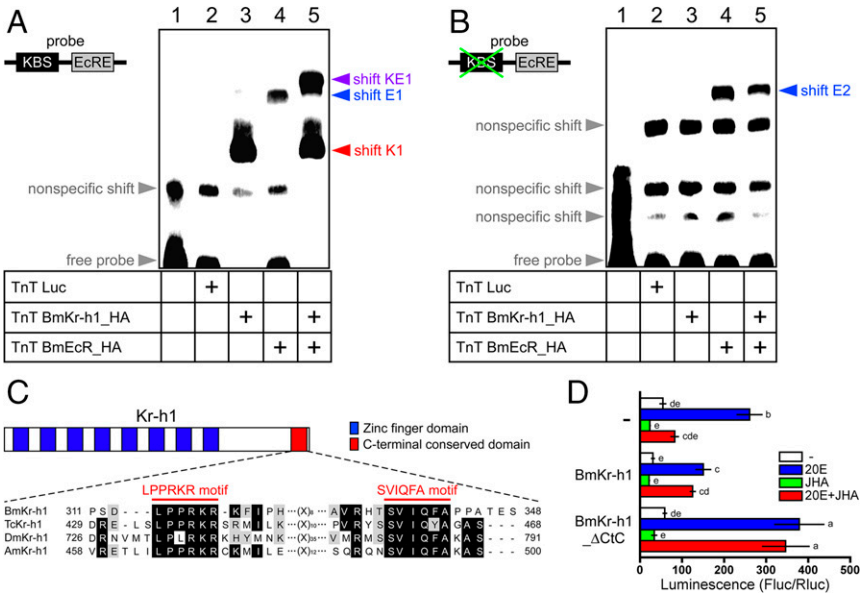

Fig. 5. Molecular mechanism of BmKr-h1-mediated transcriptional repression. Concomitant BmKr-h1 and BmEcR binding was examined by EMSA with (*A*) WT and (*B*) KBS-mutated probes. (*C*) Schematic representation of the Kr-h1 structure and sequence alignment. Blue and red boxes indicate the zinc finger and CtC domains, respectively. Alignment of predicted amino acid sequences in the BmKr-h1 C terminus with those of *T. castaneum* Kr-h1 (TcKr-h1; GenBank accession no. NP_001129235), *D. melanogaster* Kr-h1 (DmKr-h1; GenBank accession no. NP_477467), and *Apis mellifera* Kr-h1 (AmKr-h1; GenBank accession no. AB642243). Black and light gray shading indicate identical and similar amino acid residues, respectively. Red bars indicate the putative protein interaction motifs (LPPRKR and SVIQFA) in the CtC domain. (*D*) Reporter assays using BmKr-h1 constructs lacking the CtC domain were performed to characterize CtC domain function. BmKr-h1_ΔCtC refers to BmKr-h1 with the CtC domain deleted. NIAS-Bm-aff3 cells were cotransfected with a reporter plasmid carrying the *BmE93A* promoter region (−2909 to +290), a reference reporter plasmid, and the mutated BmKr-h1 expression plasmid. The cells were treated with 1 μM 20E and 10 μM JHA for 2 d, and reporter activity was measured by using a dual-luciferase reporter assay system. Data represent means ± SD (n = 3). Bars with the same letter are not significantly different (Tukey–Kramer test, α = 0.05).

whereas a specific shift band (shift E2) was observed with BmEcR_HA alone (Fig. 5*B*, lane 4) and with the combination of BmKr-h1 and BmEcR (Fig. 5*B*, lane 5). These results clearly indicate that BmKr-h1 and BmEcR independently bind to the KBS and EcRE, respectively, and that these two factors could simultaneously bind the adjacent sequences to form shift KE1. Therefore, our first hypothesis that physical interference occurs between BmKr-h1 and BmEcR on the *BmE93A* promoter is unlikely.

More than 60% of BmKr-h1 is composed of zinc finger domains, and the remaining 40% shares no similarity with other insect Kr-h1s (15, 17). However, we discovered two distinctive motifs (LPPRKR and SVIQFA motif) in the Kr-h1 C terminus conserved in four holometabolous insects and termed this region the C-terminal conserved domain (CtC domain; Fig. 5*C*). To determine whether the CtC domain is involved in the transcriptional inhibitory activity of BmKr-h1, we performed reporter assays in NIAS-Bm-aff3 cells ectopically expressing WT BmKr-h1 or BmKr-h1 with deletion of the CtC domain (BmKr-h1_ΔCtC). Notably, ectopic expression of native BmKr-h1 repressed the 20E-dependent activation of a reporter carrying the −2909 to +290 region of *BmE93A* (Fig. 5*D*). In contrast, deletion of the CtC domain abolished the repression by BmKr-h1, and ectopic expression of BmKr-h1_ΔCtC inhibited the JH-mediated repression through a dominant-negative effect (Fig. 5*D*). Taken together, these findings support that the CtC domain in Kr-h1 contributes to JH-inducible transcriptional repression of target genes.

Discussion

The pupal stage in holometabolous insects is an important intermediary for the transition from larvae to adults. *E93* gene expression during the pupal stage functions as an adult specifier and plays a key role in inducing programmed cell death necessary for tissue remodeling (30–33). Genetic studies have revealed that during the larval stage, JH suppresses *E93* expression to prevent larvae from undergoing precocious metamorphosis to adults (34–36). In the present study, we clarified the molecular mechanism underlying the repression of *E93* by JH.

RACE and developmental expression profiling revealed that *BmE93* has distinct pupal (*BmE93A*) and adult isoforms (*BmE93B*) that differ in their transcription start sites. In experiments using cultured epidermis, *BmE93A* was induced by 20E and repressed by JH, but neither hormone affected *BmE93B* expression, indicating that differential responses to these hormones enable the varied developmental expression of *BmE93* isoforms. Given that both *BmE93* isoforms share a common ORF and are involved in programmed cell death, it is likely that *BmE93A* and *BmE93B* function to disrupt larval and pupal traits in larval–pupal and pupal–adult metamorphosis, respectively. Additionally, in *D. melanogaster*, *E93* is expressed widely in adult cells during the pupal stage and contributes to many patterning processes at the adult stage (44), suggesting that *BmE93B* might be required for the patterning process in *B. mori*.

A transient JH peak during the prepupal stage has been observed in some holometabolous insects and is suggested to prevent precocious adult development (45–47). A recent study using RNAi in *T. castaneum* showed that a peak of Kr-h1 in the prepupal stage suppressed premature *E93* induction (36). However, because all previous studies were performed using whole individuals, it remains unknown whether the suppression of *E93* by JH-induced Kr-h1 is a cell-autonomous event. In this study, by using NIAS-Bm-aff3 cells, we demonstrated that the suppression of *BmE93A* by BmKr-h1 is a cell-autonomous event. *BmE93A* expression was induced by 20E, and this induction was suppressed by JHA. This hormonal response is reminiscent of that observed in early pupal epidermal cells.

We have identified a putative KBS (−2221 to −2208) upstream of *BmE93A* that is similar to the KBS previously identified upstream of *BmBR-C* (28). Through reporter assays using a *B. mori* cell line, we confirmed that this sequence is indispensable for the JH-mediated suppression of *BmE93A*. EMSA experiments revealed that BmKr-h1 physically binds to the *BmE93A* KBS. Thus, the KBS in *BmE93A* is unequivocally a functional Kr-h1–binding sequence that mediates cell-autonomous JH-dependent suppression of *BmE93A*. Moreover, we identified a consensus KBS (TGACCTNNNNYAAC) by genome-wide ChIP-seq analysis, and the *BmE93A* KBS perfectly matches this consensus sequence. Interestingly, we previously observed that two Kr-h1 molecules were bound to the KBS in *BmBR-C* (28). In fact, subsequent analysis of this site revealed two consensus sequences, suggesting that the two BmKr-h1 molecules bind independently to the two KBSs in this region. Several amino acid residues in the α-helix of the C_2H_2 zinc finger enable its specific interaction with DNA (48). These residues in Kr-h1 are highly conserved in other insect species (15), suggesting that Kr-h1 homologs in other insects may also recognize the consensus KBS. Previous genetic analyses in some insects demonstrated that Kr-h1 represses *BR-C* and/or *E93* (25, 35, 36). Therefore, the function and mechanism by which Kr-h1 represses the transcription of *E93* and/or *BR-C* are essentially shared by a wide variety of insects.

We have identified an EcRE upstream of *BmE93A* and demonstrated that physically interacts with BmEcR and is responsible for the induction of *BmE93A* by 20E. Because the EcRE adjoins the KBS, it is plausible that BmKr-h1 bound to the KBS sterically interferes with the binding of BmEcR to the EcRE, thereby inhibiting induction of *BmE93A* by 20E; however, the findings of EMSA experiments rejected this simple hypothesis. We therefore alternatively hypothesize that *E93* suppression is caused by interaction of a corepressor with Kr-h1. For example, Kr-h1 might interact with general corepressors, such as Groucho (Gro) and C-terminal binding protein (CtBP), which recruit histone deacetylases to inhibit transcription of target genes (49, 50). However, WRPW or PXDLS motifs, which DNA-binding transcription factors use to interact with Gro and CtBP (49, 50), are absent in Kr-h1. Rather, we have identified a CtC domain, which is common in various insects. Reporter assays confirmed that this domain is necessary for BmKr-h1 to function as a transcriptional suppressor. Thus, the CtC motif likely mediates a functional interaction between Kr-h1 and an unknown corepressor.

The pupal specifier *BR-C* is differentially regulated by Kr-h1 in holometabolous insects; it is induced in response to JH-mediated Kr-h1 expression at the prepupal and pupal stages, whereas Kr-h1 represses *BR-C* during the larval stage (17, 18, 24, 25, 28, 36). The transcription factor CSL [CBF1/Su(H)/Lag-1] recruits a corepressor complex in the absence of Notch signaling to repress its target genes (51); however, Notch signaling converts the CSL repressor complex to an activator complex, resulting in transcriptional activation of the target genes (51). Thus, the flexibility of Kr-h1 action on *BR-C* regulation may result from different cofactors such as Notch signaling. Alternatively, because Kr-h1 contains two putative protein interaction motifs (LPPRKR and SVIQFA) in its CtC domain, a coactivator and corepressor might individually interact with either motif. Further exploration of Kr-h1–interacting cofactors would provide a unified understanding of its role in *BR-C* regulation.

In conclusion, this study yielded important findings on JH-dependent gene regulation during metamorphosis in holometabolous insects. We have identified a consensus KBS sequence, and JH-inducible Kr-h1 directly binds to the KBS in the *E93* promoter region and represses its transcription in a cell-autonomous manner. Moreover, we have identified a CtC motif that confers the inhibitory ability of Kr-h1. As this motif is common in holometabolous insects, further analysis

of the CtC motif would provide a deep understanding of the fundamental mechanism underlying the "status quo action" of JH, which could provide a substantial contribution to the pest management field and to the effective utilization of insects.

Materials and Methods

A detailed description of the materials and methods used in this study is provided in *SI Materials and Methods*.

Cell Lines. The NIAS-Bm-aff3 (52, 53) and BmN cell lines (Katakura) derived from the fat body and ovary of *B. mori*, respectively, were maintained at 25 °C in IPL-41 medium (Gibco, Invitrogen) containing 10% (vol/vol) FBS (HyClone).

Chemicals. Methoprene (JH analog [JHA]; SDS Biotech) was a gift from Sho Sakurai, Division of Life Sciences, Graduate School of Natural Science and Technology, Kanazawa University, Japan. The 20E was purchased from Sigma-Aldrich.

ACKNOWLEDGMENTS. This work was supported by Japan Society for the Promotion of Science KAKENHI Grants 25850230 and 16K15072 (to T.K.).

1. Riddiford LM (1994) Cellular and molecular actions of Juvenile hormone I. General considerations and premetamorphic actions. *Adv Insect Physiol* 24:213–274.
2. Ashburner M, Chihara C, Meltzer P, Richards G (1974) Temporal control of puffing activity in polytene chromosomes. *Cold Spring Harb Symp Quant Biol* 38:655–662.
3. Ashburner M (1990) Puffs, genes, and hormones revisited. *Cell* 61(1):1–3.
4. Dubrovsky EB (2005) Hormonal cross talk in insect development. *Trends Endocrinol Metab* 16(1):6–11.
5. Nakagawa Y, Henrich VC (2009) Arthropod nuclear receptors and their role in molting. *FEBS J* 276(21):6128–6157.
6. Riddiford LM (2012) How does juvenile hormone control insect metamorphosis and reproduction? *Gen Comp Endocrinol* 179(3):477–484.
7. Jindra M, Palli SR, Riddiford LM (2013) The juvenile hormone signaling pathway in insect development. *Annu Rev Entomol* 58:181–204.
8. Jindra M, Belles X, Shinoda T (2015) Molecular basis of juvenile hormone signaling. *Curr Opin Insect Sci* 11:39–46.
9. Wilson TG, Fabian J (1986) A *Drosophila melanogaster* mutant resistant to a chemical analog of juvenile hormone. *Dev Biol* 118(1):190–201.
10. Ashok M, Turner C, Wilson TG (1998) Insect juvenile hormone resistance gene homology with the bHLH-PAS family of transcriptional regulators. *Proc Natl Acad Sci USA* 95(6):2761–2766.
11. Miura K, Oda M, Makita S, Chinzei Y (2005) Characterization of the *Drosophila Methoprene-tolerant* gene product. Juvenile hormone binding and ligand-dependent gene regulation. *FEBS J* 272(5):1169–1178.
12. Charles J-P, et al. (2011) Ligand-binding properties of a juvenile hormone receptor, Methoprene-tolerant. *Proc Natl Acad Sci USA* 108(52):21128–21133.
13. Li M, Mead EA, Zhu J (2011) Heterodimer of two bHLH-PAS proteins mediates juvenile hormone-induced gene expression. *Proc Natl Acad Sci USA* 108(2):638–643.
14. Zhang Z, Xu J, Sheng Z, Sui Y, Palli SR (2011) Steroid receptor co-activator is required for juvenile hormone signal transduction through a bHLH-PAS transcription factor, methoprene tolerant. *J Biol Chem* 286(10):8437–8447.
15. Kayukawa T, et al. (2012) Transcriptional regulation of juvenile hormone-mediated induction of Krüppel homolog 1, a repressor of insect metamorphosis. *Proc Natl Acad Sci USA* 109(29):11729–11734.
16. Kayukawa T, Tateishi K, Shinoda T (2013) Establishment of a versatile cell line for juvenile hormone signaling analysis in *Tribolium castaneum*. *Sci Rep* 3:1570.
17. Minakuchi C, Zhou X, Riddiford LM (2008) *Krüppel homolog 1* (*Kr-h1*) mediates juvenile hormone action during metamorphosis of *Drosophila melanogaster*. *Mech Dev* 125(1-2):91–105.
18. Minakuchi C, Namiki T, Shinoda T (2009) *Krüppel homolog 1*, an early juvenile hormone-response gene downstream of Methoprene-tolerant, mediates its anti-metamorphic action in the red flour beetle *Tribolium castaneum*. *Dev Biol* 325(2):341–350.
19. Konopova B, Smykal V, Jindra M (2011) Common and distinct roles of juvenile hormone signaling genes in metamorphosis of holometabolous and hemimetabolous insects. *PLoS One* 6(12):e28728.
20. Lozano J, Belles X (2011) Conserved repressive function of Krüppel homolog 1 on insect metamorphosis in hemimetabolous and holometabolous species. *Sci Rep* 1:163.
21. DiBello PR, Withers DA, Bayer CA, Fristrom JW, Guild GM (1991) The Drosophila *Broad-Complex* encodes a family of related proteins containing zinc fingers. *Genetics* 129(2):385–397.
22. Kiss I, Bencze G, Fodor G, Szabad J, Fristrom JW (1976) Prepupal larval mosaics in *Drosophila melanogaster*. *Nature* 262(5564):136–138.
23. Kiss I, Beaton AH, Tardiff J, Fristrom D, Fristrom JW (1988) Interactions and developmental effects of mutations in the *Broad-Complex* of *Drosophila melanogaster*. *Genetics* 118(2):247–259.
24. Zhou X, Riddiford LM (2002) Broad specifies pupal development and mediates the 'status quo' action of juvenile hormone on the pupal-adult transformation in *Drosophila* and *Manduca*. *Development* 129(9):2259–2269.
25. Huang J, et al. (2011) DPP-mediated TGFbeta signaling regulates juvenile hormone biosynthesis by activating the expression of juvenile hormone acid methyltransferase. *Development* 138(11):2283–2291.
26. Zhou B, Hiruma K, Shinoda T, Riddiford LM (1998) Juvenile hormone prevents ecdysteroid-induced expression of broad complex RNAs in the epidermis of the tobacco hornworm, *Manduca sexta*. *Dev Biol* 203(2):233–244.
27. Muramatsu D, Kinjoh T, Shinoda T, Hiruma K (2008) The role of 20-hydroxyecdysone and juvenile hormone in pupal commitment of the epidermis of the silkworm, *Bombyx mori*. *Mech Dev* 125(5-6):411–420.
28. Kayukawa T, et al. (2016) Krüppel homolog 1 inhibits insect metamorphosis via direct transcriptional repression of *Broad-Complex*, a pupal specifier gene. *J Biol Chem* 291(4):1751–1762.
29. Baehrecke EH, Thummel CS (1995) The *Drosophila E93* gene from the 93F early puff displays stage- and tissue-specific regulation by 20-hydroxyecdysone. *Dev Biol* 171(1):85–97.
30. Lee CY, et al. (2000) *E93* directs steroid-triggered programmed cell death in *Drosophila*. *Mol Cell* 6(2):433–443.
31. Lee CY, Baehrecke EH (2001) Steroid regulation of autophagic programmed cell death during development. *Development* 128(8):1443–1455.
32. Liu H, Wang J, Li S (2014) E93 predominantly transduces 20-hydroxyecdysone signaling to induce autophagy and caspase activity in *Drosophila* fat body. *Insect Biochem Mol Biol* 45:30–39.
33. Liu X, et al. (2015) 20-Hydroxyecdysone (20E) Primary response gene *E93* modulates 20E signaling to promote *Bombyx* larval-pupal metamorphosis. *J Biol Chem* 290(45):27370–27383.
34. Ureña E, Manjón C, Franch-Marro X, Martín D (2014) Transcription factor E93 specifies adult metamorphosis in hemimetabolous and holometabolous insects. *Proc Natl Acad Sci USA* 111(19):7024–7029.
35. Belles X, Santos CG (2014) The MEKRE93 (Methoprene tolerant-Krüppel homolog 1-E93) pathway in the regulation of insect metamorphosis, and the homology of the pupal stage. *Insect Biochem Mol Biol* 52:60–68.
36. Ureña E, Chafino S, Manjón C, Franch-Marro X, Martín D (2016) The occurrence of the holometabolous pupal stage requires the interaction between E93, Krüppel homolog 1 and Broad-Complex. *PLoS Genet* 12(5):e1006020.
37. Shimomura M, et al. (2009) KAIKObase: An integrated silkworm genome database and data mining tool. *BMC Genomics* 10:486.
38. Satake S, Kaya M, Sakurai S (1998) Hemolymph ecdysteroid titer and ecdysteroid-dependent developmental events in the last-larval stadium of the silkworm, Bombyx mori: Role of low ecdysteroid titer in larval-pupal metamorphosis and a reappraisal of the head critical period. *J Insect Physiol* 44(10):867–881.
39. Calvez B, Hirn M, De Reggi M (1976) Ecdysone changes in the haemolymph to two silkworms (Bombyx mori and Philosamia cynthia) during larval and pupal development. *FEBS Lett* 72(1):57–61.
40. Kaneko Y, Takaki K, Iwami M, Sakurai S (2006) Developmental profile of annexin IX and its possible role in programmed cell death of the Bombyx mori anterior silk gland. *Zoolog Sci* 23(6):533–542.
41. Kamimura M, et al. (2012) Fungal ecdysteroid-22-oxidase, a new tool for manipulating ecdysteroid signaling and insect development. *J Biol Chem* 287(20):16488–16498.
42. Kayukawa T, et al. (2014) Hormonal regulation and developmental role of Krüppel homolog 1, a repressor of metamorphosis, in the silkworm *Bombyx mori*. *Dev Biol* 388(1):48–56.
43. Cherbas L, Lee K, Cherbas P (1991) Identification of ecdysone response elements by analysis of the *Drosophila Eip28/29* gene. *Genes Dev* 5(1):120–131.
44. Mou X, Duncan DM, Baehrecke EH, Duncan I (2012) Control of target gene specificity during metamorphosis by the steroid response gene *E93*. *Proc Natl Acad Sci USA* 109(8):2949–2954.
45. Williams CM (1961) Juvenile Hormone II. Its role in endocrine control of molting, pupation, and adult development in cecropia silkworm. *Biol Bull* 121:572–585.
46. Kiguchi K, Riddiford LM (1978) Role of juvenile hormone in pupal development of tobacco hornworm, *Manduca sexta*. *J Insect Physiol* 24:673–680.
47. Nijout HF (1994) The endocrine control of molting and metamorphosis. *Insect hormones*, ed Nijout HF (Princeton Univ Press, Princeton, NJ), pp 89–141.
48. Iuchi S (2001) Three classes of C_2H_2 zinc finger proteins. *Cell Mol Life Sci* 58(4):625–635.
49. Turner J, Crossley M (2001) The CtBP family: Enigmatic and enzymatic transcriptional co-repressors. *Bio Essays* 23(8):683–690.
50. Jennings BH, Ish-Horowicz D (2008) The Groucho/TLE/Grg family of transcriptional co-repressors. *Genome Biol* 9(1):205.
51. Borggrefe T, Oswald F (2016) Setting the stage for Notch: The *Drosophila*Su(H)-Hairless Repressor Complex. *PLoS Biol* 14(7):e1002524.
52. Imanishi S, Akiduki G, Haga A (2002) Novel insect primary culture method by using newly developed media and extracellular matrix. *In Vitro Cell Dev Biol* 38:16-A.
53. Takahashi T, et al. (2006) Calreticulin is transiently induced after immunogen treatment in the fat body of the silkworm *Bombyx mori*. *J Insect Biotechnol Sericol* 75:79–84.
54. Livak KJ, Schmittgen TD (2001) Analysis of relative gene expression data using real-time quantitative PCR and the 2(-ΔΔC(T)) method. *Methods* 25(4):402–408.
55. Sambrook J, Fritsch EF, Maniatis T (1989) Isolation of high-molecular-weight DNA from mammalian cells. Molecular Cloning: A Laboratory Manual, eds Sambrook J, Fritsch EF, Maniatis T (Cold Spring Harbor Lab Press, Cold Spring Harbor, NY), 2nd ed, pp 14–19.
56. Kanamori Y, et al. (2010) A eukaryotic (insect) tricistronic mRNA encodes three proteins selected by context-dependent scanning. *J Biol Chem* 285(47):36933–36944.
57. Bolger AM, Lohse M, Usadel B (2014) Trimmomatic: A flexible trimmer for Illumina sequence data. *Bioinformatics* 30(15):2114–2120.
58. Langmead B, Salzberg SL (2012) Fast gapped-read alignment with Bowtie 2. *Nat Methods* 9(4):357–359.
59. Zhang Y, et al. (2008) Model-based analysis of ChIP-Seq (MACS). *Genome Biol* 9(9):R137.
60. Bailey TL, et al. (2009) MEME SUITE: Tools for motif discovery and searching. *Nucleic Acids Res* 37(Web server issue):W202-8.